A Hybrid Winding Model of Disc-Type Power Transformers for Frequency Response Analysis

A. Shintemirov, W. H. Tang, *Member, IEEE*, and Q. H. Wu, *Senior Member, IEEE*

***Abstract*—The paper presents a hybrid model of disc-type power transformer winding for frequency response analysis (FRA) based on traveling wave and multiconductor transmission line (MTL) theories. Each disc of a winding is described by traveling wave equations, which are connected to each other in a form of MTL matrix model. This significantly reduces the order of the model with respect to previously established MTL models of transformer winding. The model is applied to frequency response simulation of two single-phase transformers. The simulations are compared with the experimental data and calculated results using lumped parameter and MTL models reported in other publications. It is shown that the model can be used for FRA result interpretation in an extended range of frequencies up to several mega Hertz and resonance analysis under very fast transient overvoltages (VFTOs).**

***Index Terms*—Frequency response analysis, multiconductor transmission lines, transfer functions, transformer windings.**

NOMENCLATURE

FRA	Frequency response analysis.
MTL	Multiconductor transmission line.
HV, LV	High and low voltage.
Z_{inp}, Z_{out}	Impedances of measurement cables.
l, a	Conductor length of a disc and a turn.
n	Total number of discs in winding.
x, t	Space and time coordinates.
Δx	Unit length of disc conductor.
u, i	Time and space dependant voltage and current.
s	Laplace transform operator.
ω	Angular frequency.
j	Imaginary unit.
w	Cross-sectional wight of disc conductor.
h	Cross-sectional height of disc conductor.
ε_0	Permittivity of free space.
ε_r	Relative permittivity of insulating medium.
μ_0	Magnetic permeability of free space.
τ_{t}	Insulation thickness between adjacent turns.
τ_{d}	Insulation thickness between adjacent discs.
$R_{\min \text{HV}}$	HV winding minimum radius.
$R_{\max \text{LV}}$	LV winding maximum radius (core radius if LV winding is absent).
R_{geom}	Equivalent circular radius of disc conductor.
σ_c	Conductivity of disc conductor.
I_0, I_1	Modified Bessel functions of first kind.

Winding Parameters Per Unit Conductor Length:

K_i	Average interturn capacitance of the $i\text{th}$ disc.
C_i	Average ground capacitance of the $i\text{th}$ disc.
$C_{\text{d}i(i+1)}$	Average interdisc capacitance between the $i\text{th}$ and $(i+1)\text{th}$ discs.
r_i	Average resistance of the $i\text{th}$ disc.
L_i	Average inductance of the $i\text{th}$ disc.
$M_{i(i+1)}$	Average mutual inductance between the $i\text{th}$ and $(i+1)\text{th}$ discs.
G_i	Average ground conductance of the $i\text{th}$ disc.
g_i	Average interturn conductance of the $i\text{th}$ disc.
$G_{\text{d}i(i+1)}$	Average interdisc conductance between the $i\text{th}$ and $(i+1)\text{th}$ discs.
Z_i	Impedance of the $i\text{th}$ disc.
Y_i	Admittance of the $i\text{th}$ disc.
$Y_{\text{s}i}$	Interturn admittance of the $i\text{th}$ disc.
$Q_{i(i+1)}$	Interdisc admittance between the $i\text{th}$ and $(i+1)\text{th}$ discs.
λ	Self-inductance of a disc turn.
μ	Mutual inductance between two adjacent turns.
r_{dc}	Dc resistance of the unit length conductor.

I. INTRODUCTION

AMONG various techniques applied to power transformer condition monitoring, only FRA is most suitable for reliable winding distortion and deformation assessment. It is based upon a fact that winding deviation or geometrical deformation

Manuscript received December 12, 2007; revised July 14, 2008. First published March 04, 2009; current version published March 25, 2009. This work was supported by the Center for International Programs under a Kazakhstan Presidential Bolashak Scholarship and by a Grant from JSC "Science Fund" for research at the University of Liverpool, Liverpool, U.K. Paper no. TPWRD-00805-2007.

The authors are with the Department of Electrical Engineering and Electronics, University of Liverpool, Liverpool L69 3GJ, U.K. (e-mail: qhwu@liv.ac.uk).

Digital Object Identifier 10.1109/TPWRD.2008.2007028

influences the changes of internal distances and profiles of the winding, which are related to internal capacitances and inductances. Sufficiently different values of combinations of these internal parameters reply essentially altered frequency responses, which can be observed by applying variable frequency signals to the reference point of winding and measuring output response signals [1], [2].

Despite of extensive FRA practice, transformer winding condition assessment is usually conducted by trained experts. The obtained FRA traces are compared with the references taken from the same winding during previous tests or from the corresponding winding of a "sister" transformer, or from other phases of the same transformer. The shifts in resonant frequencies and magnitude of FRA traces may indicate a potential winding deformation.

A range of research activities have been undertaken to utilize FRA in the development of suitable lumped parameter mathematical models of transformer windings, where each section of a winding represents a group of turns or discs. In [3]–[6] analytical expressions were used to estimate parameters of an equivalent lumped parameter models based on the geometry of winding. Well-known finite-element method was applied in [7] for more precise calculation of winding parameters for an equivalent circuit model. These work showed high degree of accuracy compared with experiment measurements. However, the precise simulation of high-frequency behavior of winding above 1 MHz can be achieved only with small sectioning of the models which leads to its essential complexity [8].

On the other hand, the theories of distributed parameter systems and traveling wave in transmission lines offer an appropriate mathematical foundation to model, in a compact mathematical form, the propagation processes of a voltage signal injected into a transformer winding [9]. This can be used for interpretation of FRA measurements in an extended range of frequencies up to 10 MHz. The advantages of such high frequency measurements for FRA were discussed in [10], [11], which show that FRA measurements are more sensitive to minor winding movements in the high frequency range.

In practice, distributed parameter modeling of transformer windings is based upon the application of MTL theory [12]. The theory has been employed to machine winding analysis [13] and, subsequently, transformer winding mathematical description [14]–[19] used for partial discharge location purposes and VFTOs studies. However, these models do not take into account constructional features of transformer windings. Generally, each turn of a winding is represented as a single transmission line [14]–[16], [19], which makes MTL models complex to operate in case of analysis of a winding with a large number of turns.

In this paper a novel approach to model disc-type transformer winding frequency behavior at FRA testing is presented. Firstly, injected source signal propagation along a single winding disc is considered using the analytical approach and results of the transformer winding analysis obtained by Rüdenberg [20]. Then, the derived traveling wave equations are applied for all discs of the winding and connected to each other in a matrix form of MTL model. This significantly reduces the number of equations in the model with respect to the previously established MTL models of transformer windings. Subsequently, application of the model to simulate frequency responses of an input impedance and winding resonances under VFTOs is presented. Simulation comparisons are given with the previously reported experimental and calculated results being obtained using lumped parameter and MTL models to verify the proposed model.

II. Equivalent Distributed Parameter Circuit of Transformer Winding

In this paper a continuous disc-type winding is analyzed, since it represents the essential part of HV transformer windings. Each disc of the winding consists of a number of turns wounded in a radial direction. In practice, continuous disc-type windings are wound to provide the same direction of a flowing current along all discs of a winding. In some transformers, the reinforcement of an insulation at the ends of a winding results to a reduced number of turns for a several discs closest to the winding ends. Thus, the conductor length of the extreme discs can differ from those of the middle discs. However, in this study for the sake of simplicity an equal conductor length of all winding discs is accepted.

In order to obtain a general equivalent circuit of the winding, each disc is considered as an equivalent distributed parameter circuit with turns being stretched out in radial direction of the winding, similar to an equivalent circuit of transformer winding proposed with respect to the axial direction [21]. Entering interdisc connections and taking into account above simplifications, the equivalent distributed parameter circuit of disc-type transformer winding at FRA testing can be composed as in Fig. 1.

As clear from the equivalent circuit the disc numeration is marked from the top till down and the direction of the space coordinate x is denoted from the left terminal of each disc towards the right end. Each disc has its own parameters signified by a corresponding disc number and the discs are connected to each other by a curve line. Thus, notations of $u_1(t,0)$, $i_1(t,0)$ and $u_n(t,l)$, $i_n(t,l)$ denote the voltages and currents at an input terminal and an output end of the winding, i.e., at $x=0$ for the first disc, $x=l$ for the nth disc. Note that the term "ground" in the definitions of the above capacitance C and conductance G means that the parameters can be considered as being between the winding and the core or the tank, or as interwinding in case of LV winding presence.

III. Signal Propagation Along a Winding Disc

The fundamentals of the theory of transients in coils were formulated by K.W. Wagner. He considered a coil as a transmission line with additional interturn capacitance acting between the turns [22]. The similar theoretical results were obtained by Rüdenberg [20] wherein he elaborated and extended the traveling wave theory to lossless transformer winding analysis. His results were adopted in order to include losses, associated with insulation and conductor resistance, and subsequently develop mathematical descriptions of signal propagation along a single uniform winding disc.

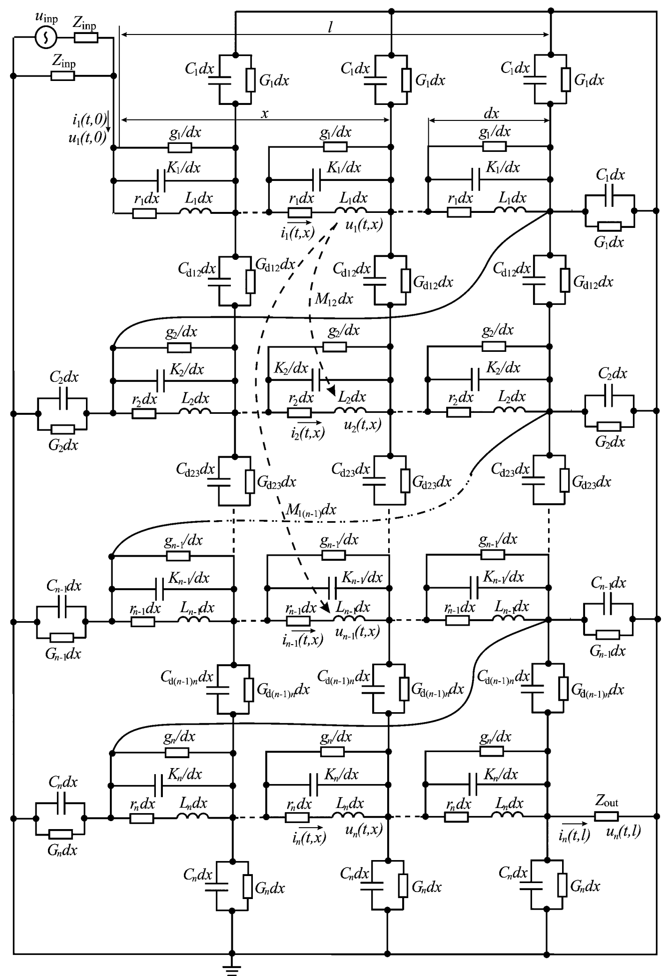

Fig. 1. Equivalent circuit of a disc-type transformer winding.

The analysis of signal propagation is based upon the Telegrapher's equations for lossy transmission lines [21], which are expressed using the notations in Fig. 1 as follows:

$$\frac{\partial i}{\partial x} = -C_{\rm g}\frac{\partial u}{\partial t} - G_{\rm g}u; \quad \frac{\partial u}{\partial x} = -L\frac{\partial i}{\partial t} - ri, \tag{1}$$

where $C_{\rm g}$ and $G_{\rm g}$ denote combined ground and interdisc capacitances and conductances, respectively, for simplicity of the analysis.

Upon these fundamental dependencies, in the following subsections the derivation of current and voltage propagation equations is presented.

A. Current Propagation Along a Winding Disc

The charging current i_{cm} for each element of disc conductor length Δx of the mth turn, flowing to "ground" due to corresponding capacitance and insulation conductance, depends on the voltage u_m of the mth turn and is described as follows:

$$i_{\rm cm} = C_{\rm g}\Delta x\frac{\partial u_m}{\partial t} + u_m \Delta x\, G_{\rm g}. \tag{2}$$

The charging current flowing from the mth turn to the $(m-1)$th one is

$$\begin{aligned} i'_{sm} &= K\Delta x\frac{\partial (u_m - u_{m-1})}{\partial t} + (u_m - u_{m-1})\Delta x\, g \\ &= K\Delta x\frac{\partial \Delta' u_m}{\partial t} + \Delta' u_m \Delta x\, g \end{aligned} \tag{3}$$

and to the $(m+1)$th turn is

$$\begin{aligned} i''_{sm} &= K\Delta x\frac{\partial (u_m - u_{m+1})}{\partial t} + (u_m - u_{m+1})\Delta x\, g \\ &= -K\Delta x\frac{\partial \Delta'' u_m}{\partial t} - \Delta'' u_m \Delta x\, g. \end{aligned} \tag{4}$$

The sum of (3) and (4) gives the total interturn current per disc conductor length Δx as follows:

$$i_{sm} = i'_{sm} + i''_{sm} = -K\Delta x\frac{\partial \Delta^2 u}{\partial t} - \Delta^2 u \Delta x\, g \tag{5}$$

where Δu is the voltage difference between adjacent turns; $\Delta^2 u$ denotes the difference of the Δu's between successive turns.

Since only interturn relations are considered, variable turn length a of a disc conductor is accepted as a unit length: $\Delta x = a$, and the second difference of voltage can be rewritten in differential form [20]

$$\Delta^2 u = a^2\frac{\Delta^2 u}{\Delta x^2} = a^2\frac{\partial^2 u}{\partial x^2}. \tag{6}$$

Substituting (6) into the sum of (2) and (5), the space derivative of the total current's decrease in the mth turn is obtained as follows:

$$\begin{aligned} -\Delta i_m = i_{\rm cm} + i_{\rm sm} &= C_{\rm g}\Delta x\frac{\partial u_m}{\partial t} + u_m \Delta x\, G_{\rm g} \\ &\quad - K\Delta x\, a^2\frac{\partial^3 u}{\partial t\, \partial x^2} - \Delta x\, g\, a^2\frac{\partial^2 u}{\partial x^2} \end{aligned} \tag{7}$$

or

$$\frac{\partial i}{\partial x} = -C_{\rm g}\frac{\partial u}{\partial t} - G_{\rm g}u + Ka^2\frac{\partial^3 u}{\partial t\, \partial x^2} + g\, a^2\frac{\partial^2 u}{\partial x^2}. \tag{8}$$

B. Voltage Propagation Along a Winding Disc

If the mth turn, having self-inductance λ per unit length, were separated from the rest of the disc, the voltage induced by the current in it would be expressed as

$$u_{\lambda m} = \lambda\Delta x\frac{\partial i_m}{\partial t} + r\Delta x\, i_m. \tag{9}$$

The two adjacent turns, coupled by the mutual inductance μ per unit length, induce a voltage in the mth turn [20]

$$\begin{aligned} u_{\mu m} &= \mu\Delta x\frac{\partial (i_{m+1} + i_{m-1})}{\partial t} \\ &= \mu\Delta x\frac{\partial\left[(i_{m+1} - i_m) - (i_m - i_{m-1}) + 2i_m\right]}{\partial t} \\ &= 2\mu\Delta x\frac{\partial i_m}{\partial t} + \mu\Delta x\frac{\partial \Delta^2 i_m}{\partial t}. \end{aligned} \tag{10}$$

Thus, as stated in [20], due to mutual inductances the induced voltages proportional to i_m are produced in the $m\mathrm{th}$ turn by each succeeding turn and, hence, it can be collected together using (9) and (10) which lead to:

$$\begin{aligned} u_{\mathrm{l}m} &= \left(\lambda + \sum \mu\right) \Delta x \frac{\partial i_m}{\partial t} + r\Delta x\, i_m \\ &= L\Delta x \frac{\partial i_m}{\partial t} + r\Delta x\, i_m, \end{aligned} \tag{11}$$

where L as defined above is the self-inductance of a disc being given per unit length and derived by total inductive effects between all turns or simply is the self-inductance of the entire disc divided by its total length [20].

Considering the interturn relationships, the second difference of current has a form of second-order space derivative:

$$\Delta^2 i = a^2 \frac{\Delta^2 i}{\Delta x^2} = a^2 \frac{\partial^2 i}{\partial x^2}, \tag{12}$$

which relates to an influence of the immediately adjacent turns, because the induced effects of other turns in a disc have already been included in (11).

The total voltage in the $m\mathrm{th}$ turn is equal to the decrease $-\Delta u_m$ which, using (10) and (11), becomes

$$-\Delta u_m = L\Delta x \frac{\partial i_m}{\partial t} + \mu a^2 \Delta x \frac{\partial^3 i_m}{\partial t\, \partial x^2} + r\Delta x\, i_m \tag{13}$$

and the voltage space derivative along the disc with aid of (12), transforms into

$$\frac{\partial u}{\partial x} = -L\frac{\partial i}{\partial t} - ri - \mu a^2 \frac{\partial^3 i}{\partial t\, \partial x^2}. \tag{14}$$

With the purpose of further processing, the last element of (14) is to be neglected within practical accuracy, since the mutual inductance μ of adjacent turns is much less than self-inductance L, which already includes mutual inductances itself.

C. Transformation Into Frequency Domain

In order to convert the above expressions (8) and (14) into frequency domain, a Laplace transform is employed. Assuming zero initial conditions

$$i(t=0,x)=0;\ u(t=0,x)=0.$$

then (8) and the simplified equation (14) are transformed into frequency domain as follows:

$$\frac{\partial U(s,x)}{\partial x} = -\, LsI(s,x) - rI(s,x); \tag{15}$$

$$\begin{aligned} \frac{\partial I(s,x)}{\partial x} = &-C_{\mathrm{g}}\, sU(s,x) - G_{\mathrm{g}} U(s,x) \\ &+ Ka^2 s \frac{\partial^2 U(s,x)}{\partial x^2} + g\, a^2 \frac{\partial^2 U(s,x)}{\partial x^2} \end{aligned} \tag{16}$$

where $U(s,x)$ and $I(s,x)$ are the Laplace transforms of the voltage $u(t,x)$ and current $i(t,x)$ correspondingly.

Thus, the derived (15) and (16) describe the injected signal propagation along a uniform winding disc in frequency domain.

IV. Mathematical Model of Transformer Winding

In order to develop a mathematical model of a disc-type transformer winding, the above obtained (15) and (16) are employed to describe signal propagation along each disc of the winding. Considering the equivalent circuit in Fig. 1, the equations include interdisc capacitances and conductances, which are subsequently combined into a matrix form similar to that of a MTL model.

The mathematical equations describing the first disc of a winding are as follows:

$$\begin{aligned} \frac{\partial U_1(s,x)}{\partial x} = &-Z_1 I_1(s,x) - sM_{12} I_2(s,x) \\ &- \cdots - sM_{1n} I_n(s,x) \end{aligned} \tag{17}$$

$$\begin{aligned} \frac{\partial I_1(s,x)}{\partial x} = &-Y_1 U_1(s,x) + a^2 Y_{\mathrm{s}1} \frac{\partial^2 U_1(s,x)}{\partial x^2} \\ &+ Q_{12} U_2(s,x) \end{aligned} \tag{18}$$

where

$$\begin{aligned} Z_1 &= L_1 s + r_1; \\ Y_1 &= (C_1 + C_{\mathrm{d}12})\, s + (G_1 + G_{\mathrm{d}12}) \\ Y_{\mathrm{s}1} &= K_1 s + g_1; \quad Q_{12} = C_{\mathrm{d}12}\, s + G_{\mathrm{d}12}. \end{aligned} \tag{19}$$

The expressions for the $i\mathrm{th}$ disc, where $i = 2, \ldots, n$ are similar to (17) and (18) with minor modifications.

The combination of the equations corresponding to all the n discs in a matrix form gives the following matrix equation:

$$\begin{aligned} \frac{\partial}{\partial x}\mathbf{U}(s,x) &= -\,\mathbf{Z}\,\mathbf{I}(s,x) \\ \frac{\partial}{\partial x}\mathbf{I}(s,x) &= -\,\mathbf{Q}\,\mathbf{U}(s,x) + \mathbf{Y_S} \frac{\partial^2}{\partial x^2}\mathbf{U}(s,x) \end{aligned} \tag{20}$$

where

$$\mathbf{Z} = \begin{bmatrix} Z_1 & sM_{12} & \cdots & sM_{1n} \\ sM_{21} & Z_2 & \ddots & \vdots \\ \vdots & \ddots & \ddots & sM_{(n-1)n} \\ sM_{n1} & \cdots & sM_{n(n-1)} & Z_n \end{bmatrix} \tag{21}$$

$$\mathbf{Q} = \begin{bmatrix} Y_1 & -Q_{12} & \cdots & 0 \\ -Q_{21} & Y_2 & \ddots & \vdots \\ \vdots & \ddots & \ddots & -Q_{(n-1)n} \\ 0 & \cdots & -Q_{n(n-1)} & Y_n \end{bmatrix} \tag{22}$$

$$\mathbf{Y_S} = \mathrm{diag}\left(a^2 Y_{\mathrm{s}1},\, a^2 Y_{\mathrm{s}2}, \ldots,\, a^2 Y_{\mathrm{s}n}\right). \tag{23}$$

The impedances and admittances Z, Y, Y_{s} of each disc and interdisc admittances Q per unit conductor length are defined as follows:

for $i = 1, \ldots, n$

$$Z_i = L_i s + r_i \text{ and } Y_{\mathrm{s}i} = K_i s + g_i, \tag{24}$$

for $i = 2, \ldots, n-1$

$$\begin{aligned} Y_i &= \left(C_i + C_{\mathrm{d}(i-1)i} + C_{\mathrm{d}i(i+1)}\right) s \\ &\quad + \left(G_i + G_{\mathrm{d}(i-1)i} + G_{\mathrm{d}i(i+1)}\right) \\ Q_{(i-1)i} &= C_{\mathrm{d}(i-1)i}\, s + G_{\mathrm{d}(i-1)i} \\ Q_{i(i+1)} &= C_{\mathrm{d}i(i+1)}\, s + G_{\mathrm{d}i(i+1)} \end{aligned} \tag{25}$$

and

$$Y_n = (C_n + C_{\mathrm{d}(n-1)n})\, s + (G_n + G_{\mathrm{d}(n-1)n}). \tag{26}$$

Equations in (20) can then be rearranged into a matrix form as follows:

$$\begin{aligned} \frac{\partial\, \mathbf{U}(s,x)}{\partial x} &= -\,\mathbf{Z}\, \mathbf{I}(s,x); \\ \frac{\partial\, \mathbf{I}(s,x)}{\partial x} &= -\,\mathbf{Q}\left(\mathbf{II} + \mathbf{Y_S Z}\right)^{-1} \mathbf{U}(s,x) \end{aligned} \tag{27}$$

or

$$\frac{\partial}{\partial x}\begin{bmatrix} \mathbf{U}(s,x) \\ \mathbf{I}(s,x) \end{bmatrix} = \mathbf{A}\begin{bmatrix} \mathbf{U}(s,x) \\ \mathbf{I}(s,x) \end{bmatrix} \tag{28}$$

where

$$\mathbf{A} = \begin{bmatrix} \mathbf{0} & -\mathbf{Z} \\ -\mathbf{Y} & \mathbf{0} \end{bmatrix} \quad \text{and} \quad \mathbf{Y} = \mathbf{Q}\left(\mathbf{II} + \mathbf{Y_S Z}\right)^{-1} \tag{29}$$

and $\mathbf{II}$ is the identity matrix, while $\mathbf{0}$ is the zero matrix.

Consequently, the following equations are derived:

$$\begin{aligned} \frac{\partial^2 \mathbf{U}(s,x)}{\partial x^2} &= \mathbf{Z}\,\mathbf{Y}\,\mathbf{U}(s,x); \\ \frac{\partial^2 \mathbf{I}(s,x)}{\partial x^2} &= \mathbf{YZ}\,\mathbf{I}(s,x). \end{aligned} \tag{30}$$

The solution of matrix (28) for the voltages and currents at the ends of transformer winding when $x = 0$ and $x = l$ is obtained in the form that follows [12]:

$$\begin{aligned} \begin{bmatrix} \mathbf{U}(s,l) \\ \mathbf{I}(s,l) \end{bmatrix} &= \mathbf{\Phi}(l)\begin{bmatrix} \mathbf{U}(s,0) \\ \mathbf{I}(s,0) \end{bmatrix} \\ &= \begin{bmatrix} \mathbf{\Phi}_{11}(l) & \mathbf{\Phi}_{12}(l) \\ \mathbf{\Phi}_{21}(l) & \mathbf{\Phi}_{22}(l) \end{bmatrix}\begin{bmatrix} \mathbf{U}(s,0) \\ \mathbf{I}(s,0) \end{bmatrix} \end{aligned} \tag{31}$$

where $\mathbf{\Phi}$ is a $2n \times 2n$ chain parameter matrix.

Since the admittance matrix $\mathbf{Y}$ is nonsymmetrical, i.e.,, $\mathbf{Y}^T \neq \mathbf{Y}$, where $\mathbf{Y}^T$ denotes the transpose of $\mathbf{Y}$, (30) are difficult to decouple in order to obtain an analytical solution using the similarity transformations as in the case of multiconductor transmission line equations [12].

On the other hand, since the turn length a varies depending on turn number in a winding disc, which affects the calculation of $\mathbf{Y}$, the matrix $\mathbf{\Phi}(l)$ can be calculated in an iterative numerical form using a matrix exponential function [12] as follows:

$$\mathbf{\Phi}(l) = \mathbf{e}^{\mathbf{A}a_p} \times \cdots \times \mathbf{e}^{\mathbf{A}a_2} \times \mathbf{e}^{\mathbf{A}a_1}, \tag{32}$$

where a_i is the turn length of the $i\mathrm{th}$ turn and p is the number of turns in a disc.

By calculating the chain parameter matrix $\mathbf{\Phi}(l)$ it is possible to derive expressions for the transformer winding transfer functions, which are presented in next section.

V. Transfer Functions of Transformer Winding for Frequency Response Analysis

In practice, frequency responses of transformer winding are obtained in a form of transfer functions of selected input or output voltages or currents with respect to the injected source voltage signal. In order to derive the expressions for transfer functions, (31) is rearranged in the form as follows:

$$\begin{bmatrix} \mathbf{I}(s,0) \\ \mathbf{I}(s,l) \end{bmatrix} = \begin{bmatrix} \mathbf{\Upsilon_{11}}(l) & \mathbf{\Upsilon_{12}}(l) \\ \mathbf{\Upsilon_{21}}(l) & \mathbf{\Upsilon_{22}}(l) \end{bmatrix}\begin{bmatrix} \mathbf{U}(s,0) \\ \mathbf{U}(s,l) \end{bmatrix} \tag{33}$$

where [12]

$$\begin{aligned} \mathbf{\Upsilon_{11}}(l) &= -\,\mathbf{\Phi_{12}}(l)^{-1}\,\mathbf{\Phi_{11}}(l); \\ \mathbf{\Upsilon_{12}}(l) &= \mathbf{\Phi_{12}}(l)^{-1} \\ \mathbf{\Upsilon_{21}}(l) &= \mathbf{\Phi_{21}}(l) - \mathbf{\Phi_{22}}(l)\,\mathbf{\Phi_{12}}(l)^{-1}\,\mathbf{\Phi_{11}}(l) \\ \mathbf{\Upsilon_{22}}(l) &= \mathbf{\Phi_{22}}(l)\,\mathbf{\Phi_{12}}(l)^{-1}. \end{aligned} \tag{34}$$

The boundary equalities for (33) derived from Fig. 1 [13] as

$$\begin{aligned} U_{i+1}(s,0) &= U_i(s,l),\ \text{for } i = 1, \ldots, n-1 \\ I_{i+1}(s,0) &= I_i(s,l),\ \text{for } i = 1, \ldots, n-1. \end{aligned} \tag{35}$$

Equation (33) can be simplified into the following form [13], [16], [19]:

$$\begin{bmatrix} I_1(s,0) \\ 0 \\ \vdots \\ 0 \\ I_n(s,l) \end{bmatrix} = \begin{bmatrix} & & \\ & \mathbf{\Upsilon}'(l) & \\ & & \end{bmatrix}\begin{bmatrix} U_1(s,0) \\ U_2(s,0) \\ \vdots \\ U_n(s,0) \\ U_n(s,l) \end{bmatrix} \tag{36}$$

where $\mathbf{\Upsilon}'(l)$ is a $(n+1) \times (n+1)$ matrix.

Finally, by inverting matrix $\mathbf{\Upsilon}'(l)$, (36) can be rewritten as follows:

$$\begin{bmatrix} U_1(s,0) \\ U_2(s,0) \\ \vdots \\ U_n(s,0) \\ U_n(s,l) \end{bmatrix} = \begin{bmatrix} & & \\ & \mathbf{\Omega}(l) & \\ & & \end{bmatrix}\begin{bmatrix} I_1(s,0) \\ 0 \\ \vdots \\ 0 \\ I_n(s,l) \end{bmatrix} \tag{37}$$

where $\mathbf{\Omega}(l) = \left[\mathbf{\Upsilon}'(l)\right]^{-1}$ is of $(n+1) \times (n+1)$ order [13].

In this research, input impedance response and transfer functions of voltages from various points of the winding are simulated and compared with the measurement results and simulations from other models. Input impedance of the winding can be found assuming a grounded winding. Thus, the following terminal condition is applied to the model:

$$U_n(s,l) = 0. \tag{38}$$

Consequently, the ratio of the input voltage signal $U_1(s,0)$ to the input current $I_1(s,0)$ gives the equation for input impedance of the winding, as follows:

$$\begin{aligned} H(s) &= \frac{U_1(s,0)}{I_1(s,0)} \\ &= \frac{\Omega_{(1,1)}\Omega_{(n+1,n+1)} - \Omega_{(1,n+1)}\Omega_{(n+1,1)}}{\Omega_{(n+1,n+1)}}. \end{aligned} \tag{39}$$

For the resonance simulation study at different positions of a winding, the transfer functions are calculated as the ratio of a voltage $U_k(s,l)$ from the end terminal of an arbitrary disc k to the input voltage signal $U_1(s,0)$ [19]

$$H(s) = \frac{U_k(s,l)}{U_1(s,0)} = \frac{\Omega_{(k+1,1)}\Omega_{(n+1,n+1)} - \Omega_{(k+1,n+1)}\Omega_{(n+1,1)}}{\Omega_{(1,1)}\Omega_{(n+1,n+1)} - \Omega_{(n+1,1)}\Omega_{(1,n+1)}}. \quad (40)$$

Using the above obtained (39) and (40), the frequency responses of the winding are simulated with the substitution $s = j\omega$. At the same time, calculations of the model parameters are performed using analytical formulae, as illustrated in the following section.

VI. Estimation of Model Electrical Parameters

Adequate estimation of the winding model parameters depends on winding geometrical dimensions and properties of winding conductor and insulation. The presence of cylindrical pressboard barriers and spacers between HV and LV windings, spacers between winding discs along with insulation oil can be accounted by an effective permittivity using the approach described in [5], [7].

Winding capacitances are estimated in a similar manner to those obtained for MTL models upon the simplified geometry of a winding, known effective permittivity of a winding insulation and adjusted per unit of disc conductor length [14]. Average interturn and interdisc capacitances K and C_{d}, respectively, are calculated using the expression for parallel plate capacitances as follows:

$$K = \frac{\varepsilon_0\varepsilon_{\mathrm{r}} h}{\tau_{\mathrm{t}}}; \quad C_{\mathrm{d}} = \frac{\varepsilon_0\varepsilon_{\mathrm{r}} w}{\tau_{\mathrm{d}}}. \quad (41)$$

An average ground capacitance C of a disc-type HV winding can be interpreted as a cylindrical capacitance between a winding and a tank, considering an external turn of a winding disc. On the contrary, for the internal turn of the disc, a ground capacitance C is calculated as the capacitance between HV and LV windings or a core

$$C = \frac{\varepsilon_0\varepsilon_{\mathrm{r}} h}{\ln\left(\frac{R_{\min \mathrm{HV}}}{R_{\max \mathrm{LV}}}\right) R_{\min \mathrm{HV}}}. \quad (42)$$

Self and mutual inductances of the winding discs L and M are calculated using the expressions derived by Wilcox [23], [24] and adjusted to per unit of disc conductor length base.

Taking into account skin effect at high frequencies, the conductor resistance r can be found using the following expressions [25]:

$$r = \mathrm{Re}\left\{ r_{\mathrm{dc}} \frac{\alpha R_{\mathrm{geom}} I_0(\alpha R_{\mathrm{geom}})}{2 I_1(\alpha R_{\mathrm{geom}})} \right\}; \; \alpha = \sqrt{(j\omega\mu_0\sigma_c)}. \quad (43)$$

The frequency-dependent conductances g, G_{d}, G are estimated using the effective loss tangents $\tan\delta$ of the corresponding insulation mediums [14], [15], [18], [19].

VII. Simulation Results and Comparison

A. Model Verification With FRA

In order to verify the model, it is applied to simulate frequency responses for a single-phase experiment transformer without a core, which consisted of a 30-double disc HV winding and a 23-turn helical LV winding, with the geometrical dimensions provided in [6]. The simulated input impedance response with aid of (39), as well as experimentally measured input impedance from the HV side of the transformer [5], are shown in Fig. 2.

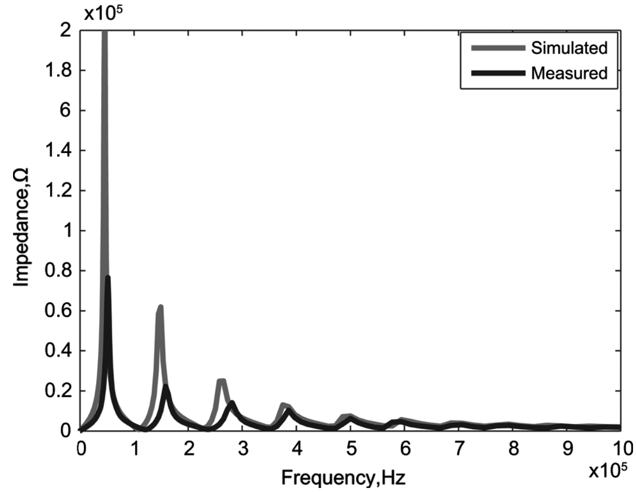

Fig. 2. Simulated with the proposed model and measured responses of open circuit impedance of the experimental transformer.

It can be observed that the simulated and measured responses are close to each other as far as the general shape and resonant frequencies are concerned. However, the most clear deviations of 10.8%, 5.57%, and 5.58% in the first three resonant frequencies, respectively, may be due to approximations of winding conductor and insulation properties accepted at the stage of parameter estimation. In addition, the developed model provides less damping at the resonant frequencies with respect to the measured response. This could be due to the existence of additional loss mechanisms [5], i.e., losses in the tank or in the conducting cylinder used to represent equipotential surface of the core, that are not considered in the proposed model, or to approximations in the expressions used for the model parameter calculation.

On the other hand, considering the input impedance response of the same experimental transformer, presented in [5] and calculated using a lumped parameter model, it is clear that the responses from both the models are almost identical to each other in terms of resonant frequencies and magnitudes. Although the developed model does not provide higher accuracy in comparison with known lumped parameter models in the frequency range up to 1 MHz, the developed model is capable of high frequency simulation with frequencies above 1 MHz, as discussed in the following subsection.

B. Winding Resonance Simulation

In practice, a FRA result interpretation includes visual cross-comparison of measured frequency responses aiming to notice newly appeared suspicious deviations of the investigated trace comparing with various etalon responses. The appearance of clear shifts in resonance frequencies or new resonant points

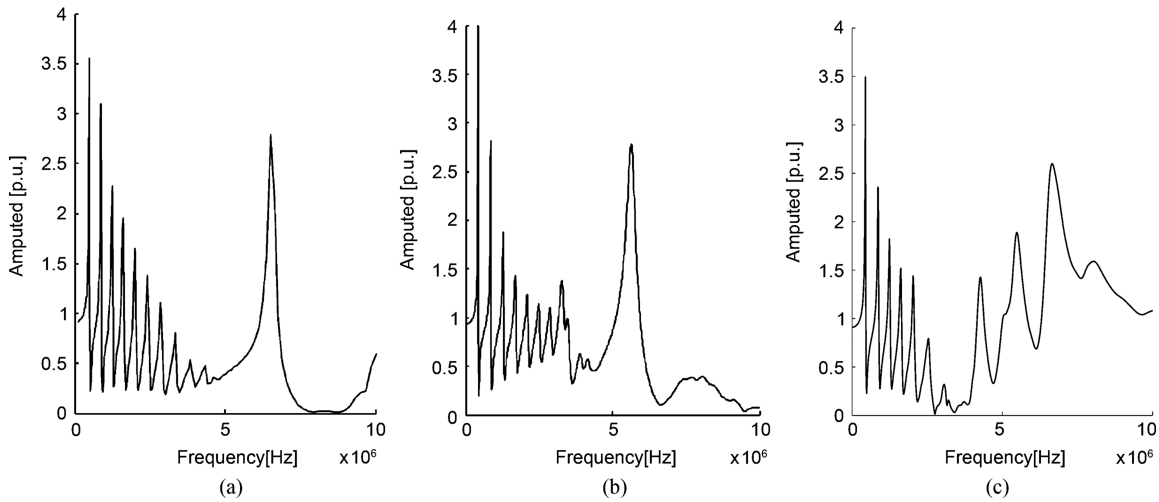

Fig. 3. Amplitudes of transfer function between the terminal of turn 20 and the input [(a) and (b) reprinted from [19]].

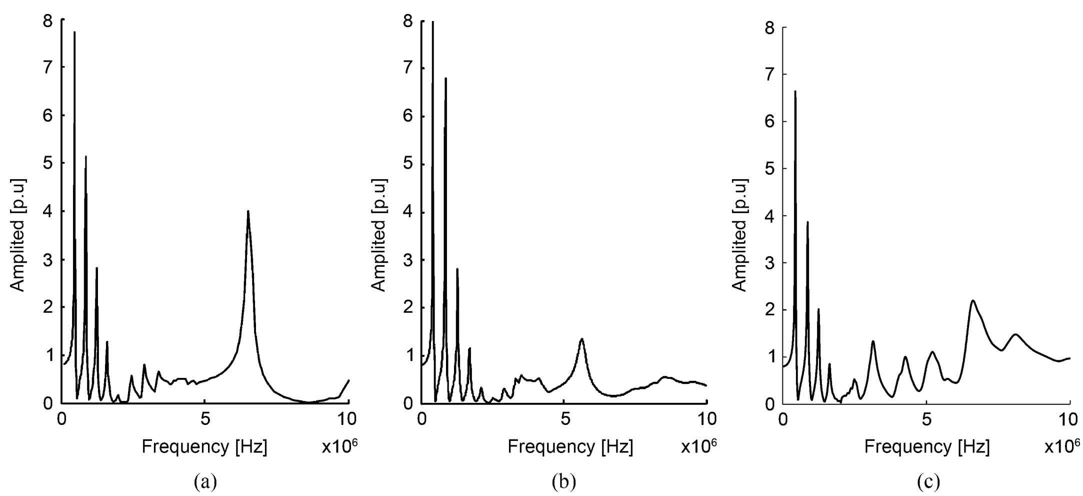

Fig. 4. Amplitudes of transfer function between the terminal of turn 40 and the input [(a) and (b) reprinted from [19]].

may characterize faulty conditions of windings. This comparative approach was extended by simulating frequency responses with lumped parameter models to analyze the effect of different winding faulty modes on deviation of resonance frequencies in comparison with the reference simulations corresponding to normal state of a winding [3]–[7]. However, the considered frequency range was limited by the reasons stated in Section I regarding the models applied. Recent work [10] showed the potential for FRA result interpretation in an extended range of frequencies up to 10 MHz, which indicates the importance of continuing the study using suitable transformer winding models. Therefore, it is necessary to investigate the proposed model correctness in a high frequency range, and a large attention should be paid, at first, to the analysis of resonance frequencies as the main sources of information about the object and secondly the ability of a model to reflect the general shape of a winding response.

Unfortunately, the reference FRA data in the frequency range of interest were not available for the analysis. However, considering that the derivation of the transfer function expressions, presented in Section V, is similar to those used for VFTOs studies with MTL models, the proposed model is employed for the comparative study using data from resonance analysis under VFTOs of an experimental transformer winding. The winding is composed of 18 discs with 10 turns per disc and its basic parameters are given in [19].

One way to analyze the resonance phenomena under very fast transients overvoltages is to compare amplitude-frequency responses of winding transfer functions measured from different points in the winding. Thus, potentially vulnerable locations in a winding, where resonance could occur, are determined [19].

Figs. 3–5 illustrate measured (a) and calculated with the MTL model frequency responses (b) of transfer functions from turns 20, 40, and 60 of the experimental transformer winding respectively, having been published in [19]. For comparison purposes, frequency responses of the transfer functions taken from the end terminals of the discs 2, 4 and 6, that correspond to turns 20, 40 and 60 of the winding respectively, are calculated using (40) and arranged in the same figures as (c). The resonant frequencies of the studied winding discs are listed in Table I.

As seen from Figs. 3–5, on the whole, the simulated frequency responses using both the MTL and developed models

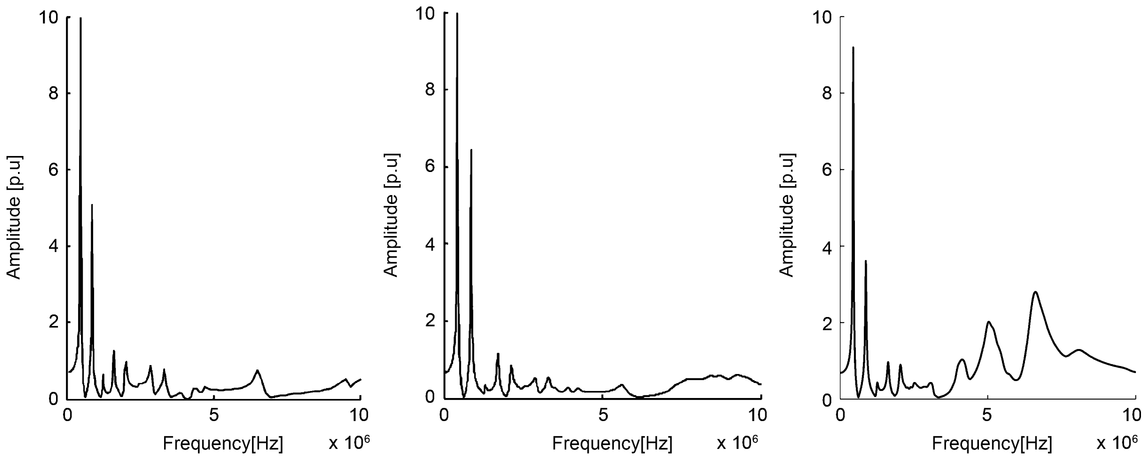

Fig. 5. Amplitudes of transfer function between the terminal of turn 60 and the input [(a) and (b) reprinted from [19]].

TABLE I
RESONANT FREQUENCIES IN DISCS 2, 4, AND 6 OF THE EXPERIMENTAL TRANSFORMER WINDING

Disc Number	Resonant Frequencies (MHz)		
	Measured [19]	**MTL model [19]**	**Proposed Model**
2	0.46 ,0.87, 1.25, 1.65, 2.0, 2.4, 2.9, 3.35, 3.8, 4.3, 6.52	0.43 ,0.86, 1.29, 1.71, 2.1, 2.52, 2.92, 3.3, 3.9, 4.15, 5.66	0.44 ,0.87, 1.24, 1.62, 2.03, 2.54 , 3.07, 3.7, 4.27, 5.49, 6.66
4	0.46 ,0.87, 1.25, 1.65, 2.4, 3.0 , 3.5, 6.5	0.43 ,0.86, 1.29, 1.71, 2.52, 2.92 , 5.66,	0.44 ,0.87, 1.25, 1.63, 2.49, 3.14 , 4.27, 5.21, 6.63,
6	0.46 ,0.87, 1.25, 1.65, 2.4, 3.0 , 3.5, 6.5	0.43 ,0.86, 1.29, 1.71, 2.12, 2.88 , 5.66,	0.44 ,0.87, 1.26, 1.63, 2.04, 2.52 , 3.08, 5.04, 6.63,

are close to measurements and correctly emphasize main resonant points of the winding. The analysis of Table I reveals that the proposed model determines the main resonant frequencies close to measurement ones in a range up to 3 MHz. In addition, a high-frequency resonance component at around 6.5 MHz frequency is more accurately located by the proposed model with respect to the MTL one, which is of the particular interest for resonance analysis [19].

However, there are deviations in resonant amplitudes and frequencies of the model responses with respect to the measured ones. It can be referred to an approximate choice of some of the experimental transformer parameters being not listed in [19] and to approximations in the expressions used for the model parameter calculation. In addition, as shown in [1], [10], [11] for the case of FRA measurements, there is an effect of ground connections and length of measurement leads on high-frequency regions of the measured responses, which also needs to be taken into account during simulation.

Comparing the two applied models, the MTL model can replicate more accurately the shape of the experimental responses, which employs a more detailed representation of the winding by the MTL model, where each turn of the winding is described by individual equations. However, this leads to a sharp increase of the order of the MTL model [19] with respect to the order of the developed model, and thus causes an additional computation complexity of the MTL model. For instance, with respect to the employed model winding, the matrix $\mathbf{\Omega}$ is of the order 19 for the developed model, whereas for the MTL model [19] the order of the corresponding matrix is 181, which is almost 9.5 times more and drastically increases computational time. Using the same computer, the calculation of the 1000 frequency points takes 26 and 333 s in MATLAB for the proposed and MTL models respectively.

It should also be mentioned that the authors' various preliminary attempts to employ a lumped parameter model for resonance simulation of the analyzed transformer winding have failed to provide high frequency resonance components at frequencies above 1 MHz due to essential discretization of the lumped model.

VIII. CONCLUSION

A novel mathematical model of disc-type transformer winding for FRA study based on the combination of traveling wave and MTL theories is presented. During the derivation of the model, each disc is represented by the traveling wave equations describing voltage signal propagation, which are then connected to each other in a form of MTL model. It allows to significantly reduce the order of the model determined only by the number of discs in a modeled winding, whereas known MTL models of transformer windings are mostly of the order of total turn number.

Using the derived transfer functions, numerical computation of frequency responses of winding input impedance and resonances under very fast transient overvoltages is undertaken. The simulations are compared with the experimental and simulation results obtained using lumped parameter and MTL models, being reported in other publications.

In the current study, only single-phase transformers without a laminated core are considered. In general, a further study needs to be undertaken to verify the model by the simulation of real transformers with core involved, which will affect calculation of the model parameters, such as inductances and ground capacitances. In this regard, different terminal connections for threephase multiwinding transformers should also be applied to investigate its effect on the model accuracy for FRA result interpretation.

The deviation of the model responses primarily concerns an inexact estimation of winding parameters, especially for correct calculation of its frequency dependant behavior. One way to overcome this difficulty is to apply evolutionary techniques for winding parameter's identification, such as Genetic Algorithms [26] and Particle Swarm Optimizer [27], etc.

In general, it is deduced that the developed model correctly reflects the interactions between capacitances and inductive elements in a disc-type power transformer winding in a wide frequency range up to several MHz. Thus, it could be used for FRA result interpretation at higher frequencies above 1 MHz, where lumped parameter models are not capable. The model is also shown to be useful for resonance analysis under VFTOs with purpose to reduce computational complexity with respect to the traditional MTL models.

Acknowledgment

The first author, A. Shintemirov, would like to thank the Center for International Programs for awarding the Kazakhstan Presidential Bolashak Scholarship and the JSC "Science Fund" for a financial grant within the frame of the "Sharyktau" competition to support his Ph.D. research at the University of Liverpool, Liverpool, U.K. He is also indebted to N. Abeywickrama and Prof. S. M. Gubanski from the Chalmers University of Technology, Göteborg, Sweden, for providing experimental data, and to Mr. H. Sun from the North China Electric Power University, Baoding, China, for valuable discussions on MTL models.

References

[1] S. A. Ryder, "Diagnosing transformer faults using frequency responce analysis," *IEEE Elect. Insul. Mag.*, vol. 19, no. 2, pp. 16–22, 2003.

[2] T. Mcgrail, *SFRA Basic Analysis Version 1.0*. Boston, MA: Doble Engineering Co, 2003, vol. 1.

[3] E. Rahimpour, J. Christian, and K. Feser, "Transfer function method to diagnose axial displacement and radial deformation of transformer windings," *IEEE Trans. Power Del.*, vol. 18, pp. 493–505, 2003.

[4] M. Florkowski and J. Furgal, "Detection of transformer winding deformations based on the transfer function- measurements and simulations," *Measur. Sci. and Technol.*, vol. 14, no. 11, pp. 1986–1992, 2003.

[5] N. Abeywickrama, Y. V. Serdyuk, and S. M. Gubanski, "Exploring possibilities for characterisation of power transfromer insulation by frequency response analysis (FRA)," *IEEE Trans. Power Del.*, vol. 21, pp. 1375–1382, 2006.

[6] N. Abeywickrama, "Effect of Dielectric and Magnetic Material Characteristics on Frequency Response of Power Transformers," Ph.D. dissertation, Chalmers Univ. Technol., Goteburg, Sweden, 2007.

[7] E. Bjerkan, "High Frequency Modelling of Power Transformers: Stresses and Diagnostics," Ph.D. dissertation, Norwegian Univ. Sci. and Technol., Trondheim, Norway, 2005.

[8] S. M. H. Hosseini, M. Vakilian, and G. B. Gharehpetian, "Comparison of transformer detailed models for fast and very transient studies," *IEEE Trans. Power Del.*, vol. 23, no. 2, pp. 733–741, Apr. 2008.

[9] A. Shintemirov and Q. H. Wu, "Transfer function of transformer winding for frequency response analysis based on traveling wave theory," in *Proc. Int. Control Conf. (ICC 2006)*, Glasgow, Scotland, Aug. 2006, p. 6.

[10] M. Wang and A. J. Vandermaar, "Improved detection of power transformer winding movement by extending the FRA high frequency range," *IEEE Trans. Power Del.*, vol. 20, pp. 1930–1938, 2005.

[11] M. Wang, A. J. Vandermaar, and K. D. Srivastava, "Transformer winding movement monitoring in service—key factors affecting FRA measurements," *IEEE Elect. Insul. Mag.*, vol. 20, no. 5, pp. 5–12, 2004.

[12] C. R. Paul, *Analysis of Multiconductor Transmission Lines*. New York: Wiley, 1994.

[13] J. L. Guardado and K. J. Cornick, "A computer model for calculating steep-front surge distribution in mashine windings," *IEEE Trans. Energy Convers.*, vol. 4, no. 1, pp. 95–101, Mar. 1989.

[14] S. N. Hettiwatte, P. A. Crosley, Z. D. Wang, A. W. Darwin, and G. Edwards, "Simulation of a transformer winding for partial discharge propagation studies," in *Proc. IEEE Power Eng. Soc. Winter Meeting*, Jan. 2002, vol. 22, pp. 1394–1399.

[15] M. S. Naderi, M. Vakilian, T. R. Blackburn, B. T. Phung, M. S. Naderi, and A. Nasiri, "A hybrid transformer model for determination of partial discharge location in transformer winding," *IEEE Trans. Dielect. Elect. Insul.*, vol. 14, no. 2, pp. 436–443, Apr. 2007.

[16] J. A. S. B. Jayasinghe, Z. D. Wang, P. N. Jarman, and A. W. Darwin, "Investigations on sensivity of FRA technique in diagnostic of transformer winding deformations," in *Proc. IEEE Int. Symp. Electrical Insulation*, Indianapolis, IN, Sep. 2004, pp. 496–499.

[17] Y. Shibuya, S. Fujita, and E. Tamaki, "Analysis of very fast transients in transformers," *IEE Proc.-Gener., Transmiss., Distrib.*, vol. 148, no. 5, pp. 377–383, 2001.

[18] M. Popov, L. van der Sluis, R. P. P. Smeets, and J. L. Roldan, "Analysis of very fast transients in layer-type transformer windings," *IEEE Trans. Power Del.*, vol. 22, no. 1, pp. 238–247, Jan. 2007.

[19] H. Sun, G. Liang, X. Zhang, and X. Cui, "Modeling of transformer windings under very fast transient overvoltages," *IEEE Trans. Electromag. Compat.*, vol. 48, no. 4, pp. 621–627, Nov. 2006.

[20] R. Rüdenberg, *Electrical Shock Waves in Power Systems: Traveling Waves in Lumped and Distributed Circuit Elements*. Cambridge, MA: Harvard University Press, 1968.

[21] L. V. Bewley, *Traveling Waves on Transmission Systems*. New York: Dover, 1963.

[22] B. Heller and A. Veverka, *Surge Phenomena in Electrical Machines*. London, U.K.: Iliffe Books, 1968.

[23] D. J. Wilcox, M. Conlon, and W. Hurley, "Calculation of self and mutual impedances for coils on ferromagnetic cores," *IEE Proc.-Sci., Measur., Technol.*, vol. 135, no. 7, pp. 470–476, 1988.

[24] D. J. Wilcox, W. G. Hurley, and M. Conlon, "Calculation of self and mutual impedances between sections of transformer windings," *IEE Proc.-Gener., Transmiss., Distrib.*, vol. 136, no. 5, pp. 308–314, 1989.

[25] W. G. Hurley and D. J. Wilcox, "Calculation of leakage inductance in transformer windings," *IEEE Trans. Power Electron.*, vol. 9, no. 1, pp. 121–126, Jan. 1994.

[26] V. Rashtchi, E. Rahimpour, and E. Rezapour, "Using a genetic algorithm for parameter identification of transformer R-L-C-M model," *Elect. Eng.*, vol. 88, no. 5, pp. 417–422, 2006.

[27] A. Shintemirov, W. H. Tang, Z. Lu, and Q. H. Wu, "Simplified transformer winding modelling and parameter identification using particle swarm optimiser with passive congregation," in *Applications of Evolutinary Computing, Lecture Notes in Computer Science 4448*. New York: Springer, 2007, pp. 145–152.

A. Shintemirov was born in 1979. He studied electrical engineering at Pavlodar State University, Pavlodar, Kazakhstan, where he received the M.Eng. and Cand.Tech.Sci. (Ph.D.) degrees in 2001 and 2004, respectively. He is currently pursuing the Ph.D. degree in the Department of Electrical Engineering and Electronics, The University of Liverpool, Liverpool, U.K.

His research interests include transformer winding modeling and evolutionary algorithm applications for transformer condition monitoring.

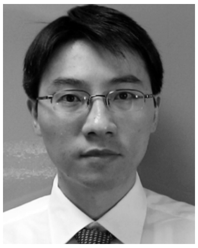

W. H. Tang (M'05) received the B.Eng. and M.Eng. degrees in electrical engineering from Huazhong University of Science and Technology, Wuhan, China, in 1996 and 2000, respectively, and the Ph.D. degree in electrical engineering from The University of Liverpool, Liverpool, U.K., in 2004.

He was a Postdoctoral Research Assistant at The University of Liverpool from 2004 to 2006. Since 2006, he has held a Lectureship in Power Engineering in the Department of Electrical Engineering and Electronics, The University of Liverpool. His research interests are transformer condition monitoring, power system operation, evolutionary computation, multiple criteria decision analysis, and intelligent decision support systems.

Q. H. Wu (M'91–SM'97) received the M.Sc. degree in electrical engineering from Huazhong University of Science and Technology (HUST), Huazhong, China, in 1981 and the Ph.D. degree in electrical engineering from The Queen's University of Belfast (QUB), Belfast, U.K., in 1987.

From 1981 to 1984, he was Lecturer of Electrical Engineering at QUB. He was a Research Fellow and Senior Research Fellow at QUB from 1987 to 1991 and a Lecturer and Senior Lecturer in the Department of Mathematical Sciences, Loughborough University, Leicestershire, U.K., from 1991 to 1995. Since 1995, he has held the Chair of Electrical Engineering in the Department of Electrical Engineering and Electronics, The University of Liverpool, Liverpool, U.K., acting as the Head of the Intelligence Engineering and Automation Group. His research interests include adaptive control, mathematical morphology, computational intelligence, information management, condition monitoring, and power system control and operation.

Dr. Wu is a Chartered Engineer and a Fellow of IEE.